

Article

# Oxygen Extraction Efficiency and Tolerance to Hypoxia in Sponges

Hans Ulrik Riisgård 

Marine Biological Research Centre, Department of Biology, University of Southern Denmark, 5300 Kerteminde, Denmark; hur@biology.sdu.dk

**Abstract:** Sponges have always been filter feeders, in contrast to all the other filter-feeding invertebrate groups for which this feeding mode is a secondary adaptation. This study calls attention to this aspect, which explains why sponges are tolerant to hypoxia, but probably not more tolerant than the other filter-feeding invertebrates. The measurement of respiration rates at decreasing oxygen concentrations along with an estimation of the oxygen extraction efficiency in the marine demosponge *Halichondria panicea* have been used to understand why sponges are tolerant to low oxygen concentrations. It was found that the respiration rate was constant down to about 1.5 mL O<sub>2</sub> L<sup>-1</sup>, which shows that the extraction efficiency increases with a decreasing oxygen concentration. It is argued that the relationship between the filtration rate and oxygen consumption in filter feeders is controlled by the resistance to the diffusion of oxygen across the boundary layer between the feeding current and the tissues of the body. A high tolerance to hypoxia is a consequence of the adaptation to filter feeding, and sponges do not have a special capacity to overcome hypoxic events.

**Keywords:** *Halichondria panicea*; filter feeding; respiration rate; filtration rate; adaptation; F/R ratio



**Citation:** Riisgård, H.U. Oxygen Extraction Efficiency and Tolerance to Hypoxia in Sponges. *J. Mar. Sci. Eng.* **2024**, *12*, 138. <https://doi.org/10.3390/jmse12010138>

Academic Editor: Caterina Longo

Received: 18 December 2023

Revised: 30 December 2023

Accepted: 8 January 2024

Published: 10 January 2024



**Copyright:** © 2024 by the author. Licensee MDPI, Basel, Switzerland. This article is an open access article distributed under the terms and conditions of the Creative Commons Attribution (CC BY) license (<https://creativecommons.org/licenses/by/4.0/>).

## 1. Introduction

Sponges (Porifera) are one of the earliest-evolved and simplest groups of animals, which developed from about 750 to 800 million years ago in a low-oxygen environment [1–3]. Today, sponges are still abundant and important organisms in many marine tropical, temperate, and polar ecosystems [4–9]. Sponges are filter feeders that generate water flow through an aquiferous system by means of flagellated cells, choanocytes [10–13]. In demosponges, one of the classes in the phylum Porifera, choanocytes are arranged in choanocyte chambers (CC) embedded in the walls between the inhalant and exhalant canals [14]. The beating flagella of the choanocytes create a flow through the inhalant and exhalant canals, and suspended food particles, mainly phytoplankton and free-living bacteria [15–17], enter the sponge through small openings (ostia) in the outer surface. Water and small particles (<3.5 μm) enter the CCs through small openings to be subsequently captured by the collar filter of the choanocytes, whereas larger particles (from 4 to 50 μm) are captured in the inhalant canals and phagocytosed [14,18,19]. The CC pump the filtered water out into an exhalant canal, and the filtered water along with waste material leaves the sponge with the exhalant jet through the exhalant opening, the osculum [19]. The feeding current also supplies the sponge with oxygen for respiration. All the currents are laminar, and oxygen in the water is taken up via diffusion, which implies that only a small fraction of the oxygen in the water pumped through the sponge is extracted for respiration under normoxic conditions, and sponges are generally very tolerant of hypoxia, which does not affect the respiration rate at very low concentrations [2,20,21]. Sponges lack conventional nerves and muscles, but they do have contractile cells, and contractile behavior is common among sponges [22–24].

The response of sponges to moderate and severe simulated hypoxic events was studied by Micaroni et al. [21]. In most sponge species, hypoxic conditions do not affect the

respiration rate at  $0.4 \text{ mg O}_2 \text{ L}^{-1}$  or a  $[0.4/9]=4.4\%$  saturated dissolved oxygen concentration. This shows that sponges can take up oxygen at very low concentrations in ambient water, thus indicating that sponges may have a “common ability to uptake oxygen at very low concentrations” in ambient water [21]. Kumala et al. [25] studied the linkage between oxygen concentration and the respiration rate of the modular demosponge *Halichondria panicea* and found that the modules scale with the sponge volume and that the maximum respiration rate increased with the sponge size with a proportionality  $\approx 1$ , suggesting that “oxygen concentration does not control the size of the sponges” and that modules enable the demosponges to grow “independent of the ambient oxygen levels” [25]. Thus, it has been hypothesized that the modular architecture has helped the evolutionary success of sponges to live in habitats where low oxygen concentrations make it impossible for other sessile, filter-feeding invertebrates to live [25]. Mills et al. [20] found that the hypoxia-inducible factor, HIF, is lacking in the sponge’s genomes, and laboratory experiments showed that *Tethya wilhelma* maintains normal transcription at oxygen levels of 0.25% modern atmospheric saturation, which is consistent with the absence of HIF. Therefore, sponges lack a signaling pathway that responds to low intracellular oxygen levels, as in more complex filter-feeding marine invertebrates. It may therefore be questioned whether sponges use a different mechanism, or whether sponges evolved at a time when less oxygen was available, and therefore, developed “an adaptive strategy to live in reduced or low-oxygen water” [21].

Choanoflagellates and sponge choanocytes share a collar of microvilli, which strain free-living bacteria and other microscopic food particles from the water current created by the beating of the flagella. The last common ancestor of the two groups was probably choanoflagellate-like, and sponges have therefore always been filter feeders [13]. This contrasts with all the other filter-feeding invertebrates for which filter feeding is a secondary adaptation, where the feeding currents often derive from respiratory currents, such as in mussels, where the feeding structures have evolved from originally respiratory gill structures [26].

The aim of this study was to call attention to this somewhat overlooked aspect, which may help to explain why sponges are tolerant to low oxygen concentrations and why they may not be more tolerant to less oxygen than the other filter-feeding invertebrates. The measurements of respiration rates at decreasing oxygen concentrations along with an estimation of the oxygen extraction efficiency in *Halichondria panicea* explants have been used to understand why sponges are tolerant to low oxygen concentrations.

## 2. Materials and Methods

The marine demosponge *Halichondria panicea* was collected in an inlet to Kerteminde Fjord, Denmark, on January 2018. Sponge cuttings of  $1 \text{ cm}^3$  (1 mL) were placed on glass slides and kept in a flow-through aquarium ( $23.0 \pm 0.9$  psu). After a week, the sponge explants attached themselves to the glass slide and had developed a single osculum, indicating a re-arranged and normal functioning aquiferous system.

The filtration rate of a sponge explant was determined using the clearance method [27]. For 100% particle retention efficiency, the volume of water cleared of suspended algal cells (*Rhodomonas salina*) per unit of time (=clearance rate) is identical to the filtration rate. In the filtration experiment, *R. salina* cells were added to the experimental chamber ( $V = 250 \text{ mL}$ ) with seawater (20 psu) under constant stirring with and without (=control) a sponge explant. The subsequent decrease in *R. salina* cell concentration was measured during 70 min by taking water samples (10 mL) every 10 min for measurements of the algal concentration using an electronic particle counter (Elzone 5380). The filtration rate was determined from the slope ( $b$ ) of a linear regression line in a semi-ln plot of the algal concentration over time, as  $F = b \times V$ . Parallel to taking water samples, the osculum cross-sectional area (OSA) of the sponge explant was recorded in 10 min intervals with an underwater camera (LH Camera Underwater Video Systems).

The oxygen consumption of a starving sponge explant was measured using an Optical Oxygen Meter System (FireStingO<sub>2</sub>, Pyro Science) in a closed respiration chamber

( $V = 115 \text{ mL}$ ) with sterile filtered ( $0.2 \mu\text{m}$ ) seawater ( $20 \text{ psu}$ ) under constant stirring. The respiration rate ( $R$ ) of the sponge explant, along with a parallel control without the explant, was determined for each 10 min interval from the slope of the linear decrease in dissolved oxygen and measured at concentrations approximating 100, 75, 50, 25, and 0% saturation in 10 s intervals for at least 60 min after the stepwise reduction in oxygen concentration by the explant. After recovery from  $\sim 0\%$  dissolved oxygen over 24 h in bio-filtered seawater, the respiration rate was again measured at 100% air saturation.

When the filtration rate ( $F, \text{L H}_2\text{O h}^{-1}$ ) and the respiration rate ( $R, \text{mL O}_2 \text{ h}^{-1}$ ) were measured, and the  $F/R$  ratio expresses the liters of water filtered per milliliter of oxygen consumed ( $\text{L H}_2\text{O (mL O}_2)^{-1}$ ). The oxygen extraction efficiency ( $EE, \%$ ) can subsequently be estimated as the reciprocal of the total amount of oxygen passing through the sponge per mL of oxygen taken up. Thus, the total amount of oxygen passing through the sponge =  $F$  multiplied  $\times$  oxygen concentration  $[\text{O}_2]_{\text{conc}}$  in the inhalant water, and the extraction efficiency was calculated as:

$$EE = 1/(F \times [\text{O}_2]_{\text{conc}}) \times 100 \tag{1}$$

The following conversion factors were used:  $1 \text{ mg O}_2 = 0.7 \text{ mL O}_2$ ; maximum oxygen concentration =  $[\text{O}_2] = 9 \text{ mg O}_2 \text{ L}^{-1} = 6.3 \text{ mL O}_2 \text{ L}^{-1}$ .

### 3. Results

The filtration rate of the *Halichondria panicea* explant was measured to be  $F = 0.12 \text{ L h}^{-1}$ , with a mean  $OSA = 0.9 \text{ mm}^2$  (Figure 1, Table 1). These values were inserted in Table 2, which also shows respiration rates at various oxygen concentrations and the estimated oxygen extraction efficiency. Figure 2 shows the respiration rate at stepwise reduced oxygen concentrations. The respiration rate is constant down to about  $1.5 \text{ mL O}_2 \text{ L}^{-1}$ , whereupon it rapidly decreases to  $0.3 \text{ mL O}_2 \text{ L}^{-1}$  before it recovers under normoxic conditions. This indicates that the extraction efficiency ( $EE$ ) increases with a decreasing oxygen concentration, as evident from Figure 3.

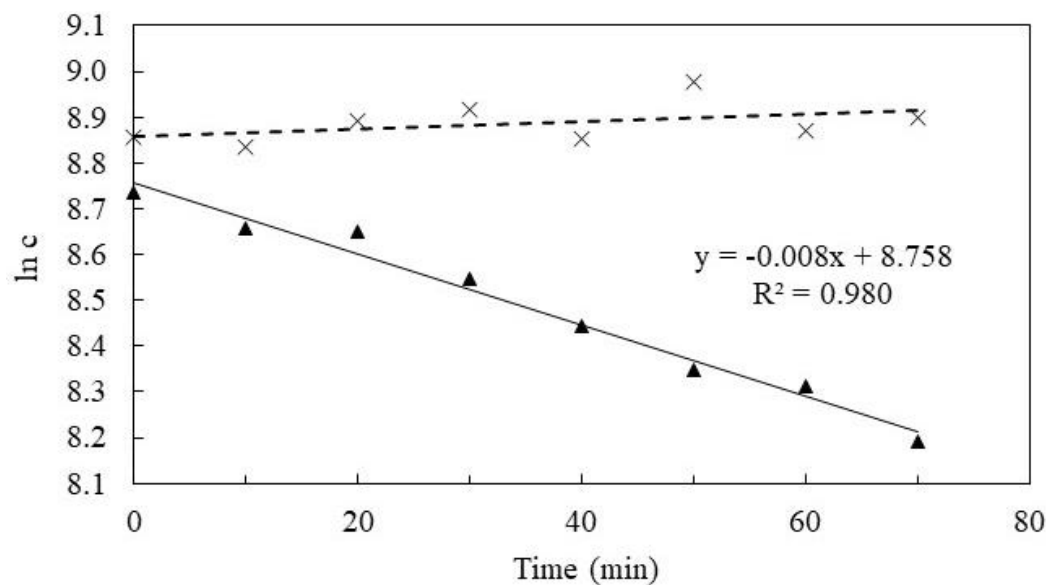


**Figure 1.** *Halichondria panicea*. Semi-ln plot of the reduction in algal concentration  $c$  ( $\text{cells mL}^{-1}$ ) (triangles) by a single-osculum sponge explant (Table 1). Linear regression function, its equation, and data (crosses) from a control experiment without sponge are shown.

**Table 1.** *Halichondria panicea*.  $V$  = body volume of explant =  $V$ ;  $V_{ch}$  = volume of experimental chamber with air mixed with seawater;  $c_0$  = initial algal concentration in clearance experiment (Figure 1);  $b$  = slope of linear regression in semi-ln plot (Figure 1);  $OSA$  = mean ( $\pm$ SD) cross-sectional osculum area of sponge explant;  $F$  ( $=b \times V$ ) = measured filtration rate;  $F_1$  = estimated filtration rate based on ([28], Figure 4 therein);  $F_2$  = estimated filtration rate based on ([29], Figure 2 therein).

$V$ (mL)	$V_{ch}$ (mL)	$c_0$ (Cells mL <sup>-1</sup> )	$b$ (min <sup>-1</sup> )	$OSA$ (mm <sup>2</sup> )	$F$ (L h <sup>-1</sup> )	$F_1$ (L h <sup>-1</sup> )	$F_2$ (L h <sup>-1</sup> )
1.0	250	6209	0.008	0.9 $\pm$ 0.4	0.12	0.08	0.16

**Table 2.** *Halichondria panicea*. Oxygen consumption by a sponge explant (ID# 2) in a closed chamber with sterile filtered seawater ( $V = 115$  mL; 20 psu) during exposure to stepwise reduced oxygen concentrations and after recovery (\*) under normoxic conditions;  $T$  = water temperature;  $(O_2)$ : mean ( $\pm$ SD) dissolved oxygen concentration (1 mg O<sub>2</sub> = 0.7 mL O<sub>2</sub>; 100% saturation corresponds to 9 mg O<sub>2</sub> L<sup>-1</sup>);  $b$  = slope ( $\pm$ SD) of linear regression of reduction in dissolved oxygen over time;  $R$  [ $=b \times V$ ] = respiration rate;  $F$  = measured filtration rate (Table 1);  $EE$  [ $=1/(F/R \times [O_2])$ ] = oxygen extraction efficiency.

Step #	$T$ (°C)	$[O_2]$ (mg L <sup>-1</sup> )	$(O_2)$ (mL L <sup>-1</sup> )	$(O_2)$ (%)	$b$ (mg O <sub>2</sub> L <sup>-1</sup> h <sup>-1</sup> )	$R$ (mg O <sub>2</sub> h <sup>-1</sup> )	$R$ (mL O <sub>2</sub> h <sup>-1</sup> )	$F$ (L h <sup>-1</sup> )	$F/R$ (L (mL O <sub>2</sub> ) <sup>-1</sup> )	$EE$ (%)
1	15.3	7.7 $\pm$ 0.6	5.4 $\pm$ 0.4	85.0 $\pm$ 6.3	0.612 $\pm$ 0.340	0.070	0.049	0.12	2.45	7.6
2	15.5	5.7 $\pm$ 0.7	4.0 $\pm$ 0.5	62.9 $\pm$ 7.5	0.656 $\pm$ 0.093	0.075	0.053	0.12	2.26	11.0
3	15.5	3.4 $\pm$ 0.7	2.4 $\pm$ 0.5	37.4 $\pm$ 7.5	0.726 $\pm$ 0.059	0.084	0.059	0.12	2.03	20.5
4	15.6	1.5 $\pm$ 0.4	1.1 $\pm$ 0.3	17.0 $\pm$ 4.3	0.493 $\pm$ 0.154	0.057	0.040	0.12	3.00	30.3
5	15.6	0.4 $\pm$ 0.0	0.3 $\pm$ 0.0	4.3 $\pm$ 0.4	0.197 $\pm$ 0.016	0.023	0.016	0.12	7.50	44.4

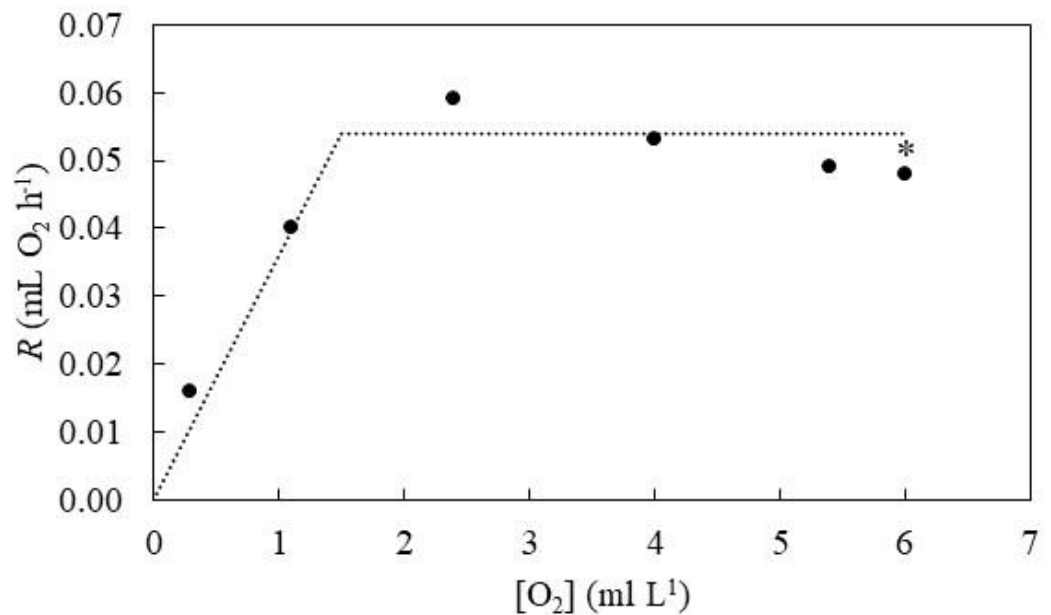


**Figure 2.** *Halichondria panicea*. Respiration rate ( $R$ ) of single-osculum explant exposed under stepwise reduced oxygen concentrations. The dotted lines indicate a suggested constant respiration rate down to about 1.5 mL O<sub>2</sub> L<sup>-1</sup>. The respiration rate after 24 h recovery from 0.3 mL O<sub>2</sub> L<sup>-1</sup> is indicated by \*. Data from Table 2.

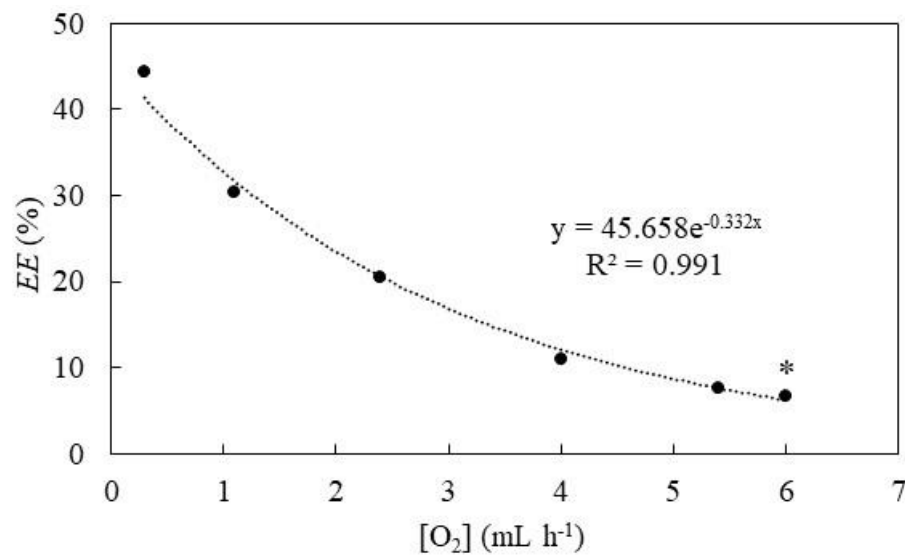


**Figure 3.** *Halichondria panicea*. Oxygen extraction efficiency ( $EE$ ) of a single-osculum explant under stepwise reduced dissolved oxygen concentrations ( $O_2$ ) (Step #1 to #5) and after 24 h recovery from  $0.3 \text{ mL } O_2 \text{ L}^{-1}$  is indicated by \*. Data from Table 2.

#### 4. Discussion

##### 4.1. Oxygen Extraction Efficiency

According to [26], the oxygen extraction efficiency ( $EE$ ) is 1% or lower in coastal filter feeders. In this study, the  $EE$  was found to be higher, between 6.7 and 7.6% under normoxic conditions (Table 1), which is likely due to the reduced filtration rates under the suboptimal experimental conditions. However, the  $F$  value is comparable to the other filtration rates measured among the *Halichondria panicea* explants (see  $F_1$  and  $F_2$  in Table 1). In another study on multi-modular *H. panicea* by [27], the  $F/R$  ratio was found to be  $15.5 \text{ L (mL } O_2)^{-1}$  or about 6 times higher than in this study, and in this case, the extraction efficiency is estimated at  $EE = 1/(15.5 \times 6.0) \times 100 = 1.1\%$ . Although the present  $F/R$  ratios do not represent an optimally filtering sponge, the patterns seen in Figures 2 and 3 represent the general trends that apply to sponges. This means that the respiration rate is constant and uninfluenced by the oxygen concentration down to about  $1.5 \text{ mL } O_2 \text{ L}^{-1}$ . Below this, the respiration decreases further down to  $0.3 \text{ mL } O_2 \text{ L}^{-1}$  without killing the sponge, as evident from its recovery under subsequent normoxic conditions (Figure 2). The constant respiration rate during decreasing oxygen concentrations also seen by ([25], Figure 2B therein), can be explained by the simultaneous increase in the oxygen extraction efficiency (Figure 3).

In the blue mussel *Mytilus edulis* the gills have turned into big filter-feeding structures, causing a many-fold increase in ventilation, and [26] interpreted the relationship between the filtration rate and oxygen consumption in terms of resistance to the diffusion of oxygen across the boundary layer at the interphase between the feeding current and body surface. At high filtration rates, the boundary layer in *M. edulis* and the filter-feeding polychaete *Urechis caupo* is about  $100 \mu\text{m}$  thick [26], and the same principle applies to sponges and all the other invertebrate filter feeders.

The ratio filtration rate/respiration rate =  $F/R$ , which expresses the liters of water filtered per mL of  $O_2$  consumed; this has been used as a tool to characterize filter feeding. In general,  $F/R > 10 \text{ L (mL } O_2)^{-1}$  is a minimum to ensure the survival of filter feeders (sponge, bryozoans, polychaetes, bivalves, ascidians, lancelets, and crustaceans) inhabiting marine waters [27,30–32]. The  $F/R$  ratio has been estimated for several sponge species by [33], and all the ratios were well above the minimum reference value of  $10 \text{ L (mL } O_2)^{-1}$ . Therefore, according to Equation (1), the extraction efficiency of marine filter-feeding invertebrates is, in general, less than  $EE = [1/(10 \times 6.3)] = 1.6\%$ . This low extraction value

explains why sponges and the other filter-feeding invertebrates (bryozoans, polychaetes, bivalves, ascidians, and lancelets) are generally tolerant to low oxygen concentrations. The next section serves as an example by comparing sponges with mussels; both are common in hypoxic bottom waters.

#### 4.2. Oxygen Uptake in Sponges versus Mussels

The respiration rate of *Halichondria panicea* is uninfluenced by decreasing oxygen concentrations until very low concentrations (Figure 2) because the oxygen retention efficiency (*EE*) increases with a decreasing oxygen concentration (Figure 3). The large water-pumping and particle-capturing gills of the blue mussel *Mytilus edulis* are oversized for respiratory purposes, and the respiration rate is therefore rather insensitive to decreasing oxygen concentrations because the mussel responds to low oxygen concentrations by increasing the *EE* ([26], Figure 10 therein). Tang and Riisgård [33] measured the oxygen uptake of *M. edulis* at various oxygen concentrations and found that a mussel exposed to oxygen concentrations decreasing from 9 to 2 mg O<sub>2</sub> L<sup>-1</sup> reduced its respiration rate only to a minor extent, while the filtration rate remained high and constant. However, below 2 mg O<sub>2</sub> L<sup>-1</sup>, the mussel responded by gradually closing its valves, resulting in a rapid decrease in the filtration rate, concurrent with a reduction of respiration rate. Further, Tang and Riisgård [34] showed that *M. edulis* during starvation periods regulate the opening degree of their valves in such a way that the oxygen concentration in the mantle cavity is reduced to minimize respiration, and at the same time, prevent anaerobic metabolism, which is energetically expensive. Typically, a starving mussel closes its valves for a certain period, followed by a short period when it re-opens, which results in the alternating fall and rise of the oxygen concentration in the mantle cavity, and therefore, an efficient mechanism, allowing the mussel to save energy. This physiological regulatory mechanism was tested by Riisgård and Larsen [35] who measured the actual body weight loss of mussels during a long-term starvation period, and subsequently compared this loss with the estimated body weight loss, assuming that the respiration rate was like that of fully open and filtering mussels. The authors found that the actual weight loss was from 10 to 12 times lower than the estimated respiratory weight loss. Thus, the physiological regulation of the valve-opening degree allows mussels to survive long periods of starvation. A similar energy-saving mechanism does not exist in the much simpler sponges, although they can close their oscula, which, in small explants, generates intrinsic deoxygenation and an oxygen gradient with increasing concentrations towards the explant periphery [36]. When the mussels are exposed to oxygen-free seawater, they close their valves completely, and the mussels may survive anoxic events by the closure and anaerobic metabolism but will fully re-open in oxygenated water after 20 min [37]. Sponges cannot tolerate oxygen-free water, and their lethal oxygen threshold is lower than 0.4 mg O<sub>2</sub> L<sup>-1</sup> [22], as also shown in this study, where the strongly reduced respiration rate recovers under normoxic conditions (Figure 2).

#### 5. Conclusions

It can be concluded that the relationship between the filtration rate and oxygen consumption in sponges and another filter-feeding invertebrate, exemplified by blue mussels, is controlled by the resistance to the diffusion of oxygen across the boundary layer between the feeding current and the tissues of the body [26]. A high tolerance to hypoxia is, therefore, a consequence of adaptation to filter feeding, and sponges do not have an “exceptional adaptive capacity” derived from their “ancient evolutionary origin” to overcome hypoxic events, as suggested by [22]. However, as proposed by Mills et al. [20], sponges, being the last common ancestor of all living animals, may have metabolized aerobically under very low environmental oxygen concentrations due to their filter-feeding mode and simple construction plan, without a muscular heart-pump-driven circulatory system with blood cells to carry oxygen from the respiratory organs to tissues and organs deep inside a complex body. Mills et al. [20] found that the hypoxia-inducible factor, HIF, is



lacking in the sponges' genomes because sponges have never had a need for a signaling pathway that responds to less intracellular oxygen. Kumala et al. [37] hypothesized that modular growth enables demosponges to grow "independent of the ambient oxygen levels" because the respiration rate increases with sponge size with a proportionality  $\approx 1$ . However, as pointed out by Riisgård and Larsen [36], sponge modules only grow to a certain size due to increasing frictional resistance in the increasingly longer inhalant and exhalant canals. Further, the increasing relative content of water in the canals compared to sponge body tissue places an upper limit on the size of the module before the structure may collapse. Thus, for a sponge to further increase in size, new modules must be formed, and in this way, multi-oscular sponges consist of single-osculum modules that have reached their maximal size, and hence, their maximal filtration rate ( $F$ ), which implies the scaling  $F/V = \text{constant}$  because  $V = \text{number of modules} \times \text{volume of a module}$  ([25], Figure 3 therein; [38], Figure 2 therein). This also implies that both  $F$  and  $R$  (respiration rate) increase linearly with  $V$  in multi-oscular sponges, and further, that growth is exponential, which is in agreement with the bioenergetic growth model presented by Riisgård and Larsen [38].

**Funding:** This work was supported by VILLUM FONDEN (grant number 40834).

**Institutional Review Board Statement:** Not applicable.

**Informed Consent Statement:** Not applicable.

**Data Availability Statement:** Data will be made available on request.

**Acknowledgments:** Thanks are given to Josephine Goldstein for the technical assistance and help with data analysis and to Florian Lüsrow for the comments on the manuscript.

**Conflicts of Interest:** The author declares no conflict of interest.

## References

1. Dohrmann, M.; Wörheide, G. Dating early animal evolution using phylogenomic data. *Sci. Rep.* **2017**, *7*, 3599. [[CrossRef](#)] [[PubMed](#)]
2. Leys, S.P.; Kahn, A.S. Oxygen and energetic requirements of the first multicellular animals. *Integ. Comp. Biol.* **2018**, *58*, 666–676. [[CrossRef](#)] [[PubMed](#)]
3. Canfield, D.E.; van Zuilen, M.A.; Nabhan, S.; Bjerrum, C.J.; Zhang, S.; Wang, H.; Wang, X. Petrographic carbon in ancient sediments constrains Proterozoic Era atmospheric oxygen levels. *Proc. Natl. Acad. Sci. USA* **2021**, *118*, e2101544118. [[CrossRef](#)] [[PubMed](#)]
4. Ayling, A.L. Factors affecting the spatial distributions of thinly encrusting sponges from temperate waters. *Oecologia* **1983**, *60*, 412–418. [[CrossRef](#)]
5. Barthel, D. On the ecophysiology of the sponge *Halichondria panicea* in Kiel Bight. II. Biomass, production, energy budget and integration in environmental processes. *Mar. Ecol. Prog. Ser.* **1988**, *43*, 87–93. [[CrossRef](#)]
6. Bell, J.J. The functional roles of marine sponges. *Estuar. Coast. Shelf Sci.* **2008**, *79*, 341–353. [[CrossRef](#)]
7. Bell, J.J.; McGrath, E.; Kandler, N.M.; Marlow, J.; Beepat, S.S.; Bachtiar, R.; Shaffer, M.R.; Mortimer, C.; Micaroni, V.; Mobilia, V.; et al. Interocean patterns in shallow water sponge assemblage structure and function. *Biol. Rev.* **2020**, *95*, 1720–1758. [[CrossRef](#)] [[PubMed](#)]
8. Van Soest, R.W.M.; Boury-Esnault, N.; Vacelet, J.; Dohrmann, M.; Erpenbeck, D.; De Voogd, N.J.; Santodomingo, N.; Bart Vanhoorne, B.; Kelly, M.; Hooper, J.N.A. Global diversity of sponges (Porifera). *PLoS ONE* **2012**, *7*, e35105. [[CrossRef](#)]
9. Morganti, T.M.; Ribes, M.; Moskovich, R.; Weisz, J.B.; Yahel, G.; Coma, R. In situ pumping rate of 20 marine demosponges is a function of osculum area. *Front. Mar. Sci.* **2021**, *8*, 583188. [[CrossRef](#)]
10. Bergquist, P.R. *Sponges*; University of California Press: Berkeley, CA, USA; Los Angeles, CA, USA, 1978; 268p.
11. Simpson, T.L. *The Cell Biology of Sponges*; Springer-Verlag: New York, NY, USA, 1984.
12. Lavrov, A.I.; Bolshakov, F.V.; Tokina, D.B.; Ereskovsky, A.V. Fine details of the choanocyte filter apparatus in asconoid calcareous sponges (Porifera: Calcarea) revealed by ruthenium red fixation. *Zoology* **2022**, *150*, 125984. [[CrossRef](#)]
13. Nielsen, C. Hydrodynamics in early animal evolution. *Biol. Rev.* **2023**, *98*, 376–385. [[CrossRef](#)] [[PubMed](#)]
14. Weissenfels, N. The filtration apparatus for food collection in freshwater sponges (Porifera, Spongillidea). *Zoomorphology* **1992**, *112*, 51–55. [[CrossRef](#)]
15. Reiswig, H.M. Particle feeding in natural populations of three marine demosponges. *Biol. Bull.* **1971**, *141*, 568–591. [[CrossRef](#)]
16. Reiswig, H.M. The aquiferous systems of three marine Demospongiae. *J. Morphol.* **1975**, *145*, 493–502. [[CrossRef](#)] [[PubMed](#)]

17. Luskow, F.; Riisgård, H.U.; Solovyeva, V.; Brewer, J.R. Seasonal changes in bacteria and phytoplankton biomass control the condition index of the demosponge *Halichondria panicea* in temperate Danish waters. *Mar. Ecol. Prog. Ser.* **2019**, *608*, 119–132. [[CrossRef](#)]
18. Imsiecke, G. Ingestion, digestion, and egestion in *Spongilla lacustris* (Porifera, Spongillidae) after pulse feeding with *Chlamydomonas reinhardtii* (Volvocales). *Zoomorphology* **1993**, *113*, 233–244. [[CrossRef](#)]
19. Funch, P.; Kealy, R.A.; Goldstein, J.; Brewer, J.R.; Solovyeva, V.; Riisgård, H.U. Fate of microplastic captured in the marine demosponge *Halichondria panicea*. *Mar. Poll. Bull.* **2023**, *194*, 115403. [[CrossRef](#)]
20. Mills, D.B.; Francis, W.R.; Vargas, S.; Larsen, M.; Elemans, C.H.P.; Canfield, D.E.; Wörheide, G. The last common ancestor of animals lacked the HIF pathway and respired in low-oxygen environments. *eLife* **2018**, *7*, e31176. [[CrossRef](#)]
21. Micaroni, V.; Strano, F.; McAllen, R.; Woods, L.; Turner, J.; Harman, L.; Bell, J.J. Adaptive strategies of sponges to deoxygenated oceans. *Glob. Change Biol.* **2022**, *28*, 1972–1989. [[CrossRef](#)]
22. Elliott, G.R.D.; Leys, S.P. Coordinated contractions effectively expel water from the aquiferous system of a freshwater sponge. *J. Exp. Biol.* **2007**, *210*, 3736–3748. [[CrossRef](#)]
23. Kealy, R.A.; Busk, T.; Goldstein, J.; Larsen, P.S.; Riisgård, H.U. Hydrodynamic characteristics of aquiferous modules in the demosponge *Halichondria panicea*. *Mar. Biol. Res.* **2019**, *15*, 531–540. [[CrossRef](#)]
24. Goldstein, J.; Funch, P. A review on genus *Halichondria* (Demospongiae, Porifera). *J. Mar. Sci. Eng.* **2022**, *10*, 1312. [[CrossRef](#)]
25. Kumala, L.; Thomsen, M.; Canfield, D.E. Respiration kinetics and allometric scaling in the demosponge *Halichondria panicea*. *BMC Ecol. Evol.* **2023**, *23*, 53. [[CrossRef](#)] [[PubMed](#)]
26. Jørgensen, C.B.; Møhlenberg, M.; Sten-Knudsen, O. Nature of relation between ventilation and oxygen consumption in filter feeders. *Mar. Ecol. Prog. Ser.* **1986**, *29*, 73–88. [[CrossRef](#)]
27. Riisgård, H.U.; Kumala, L.; Charitonidou, K. Using the F/R-ratio for an evaluation of the ability of the demosponge *Halichondria panicea* to nourish solely on phytoplankton versus free-living bacteria in the sea. *Mar. Biol. Res.* **2016**, *12*, 907–916. [[CrossRef](#)]
28. Goldstein, J.; Riisgård, H.U.; Larsen, P.S. Exhalant jet speed of single-osculum explants of the demosponge *Halichondria panicea* and basic properties of the sponge-pump. *J. Exp. Mar. Biol. Ecol.* **2019**, *511*, 82–90. [[CrossRef](#)]
29. Riisgård, H.U.; Larsen, P.S. Filtration rates and scaling in demosponges. *J. Mar. Sci. Eng.* **2022**, *10*, 643. [[CrossRef](#)]
30. Jørgensen, C.B. Comparative physiology of suspension feeding. *Ann. Rev. Physiol.* **1975**, *37*, 57–79. [[CrossRef](#)]
31. Riisgård, H.U.; Larsen, P.S. Comparative ecophysiology of active zoobenthic filter-feeding, essence of current knowledge. *J. Sea Res.* **2000**, *44*, 169–193. [[CrossRef](#)]
32. Riisgård, H.U. Filter-feeding mechanisms in crustaceans. In *Lifestyles and Feeding Biology, Volume II. The Natural History of Crustaceans*; Thiel, M., Watling, L., Eds.; Oxford University Press: Oxford, UK, 2015; Chapter 15; pp. 418–463.
33. Tang, B.; Riisgård, H.U. Relationship between oxygen concentration, respiration and filtration rate in blue mussel *Mytilus edulis*. *J. Oceanol. Limnol.* **2018**, *36*, 395–404. [[CrossRef](#)]
34. Tang, B.; Riisgård, H.U. Physiological regulation of valve-opening degree enables mussels *Mytilus edulis* to overcome starvation periods by reducing the oxygen uptake. *Open J. Mar. Sci.* **2016**, *6*, 341–352. [[CrossRef](#)]
35. Riisgård, H.U.; Larsen, P.S. Physiologically regulated valve-closure makes mussels long-term starvation survivors: Test of hypothesis. *J. Mollusc. Stud.* **2015**, *81*, 303–307. [[CrossRef](#)]
36. Lesser, M.P. Size effects on pumping rates in high microbial versus low microbial abundance marine sponges. *Oceans* **2023**, *4*, 394–408. [[CrossRef](#)]
37. Kumala, L.; Larsen, M.; Glud, R.N.; Canfield, D.E. Spatial and temporal anoxia in single-osculum *Halichondria panicea* demosponge explants studied with planar optodes. *Mar. Biol.* **2021**, *168*, 173. [[CrossRef](#)]
38. Riisgård, H.U.; Larsen, P.S. Actual and model-predicted growth of sponges—with a bioenergetic comparison to other filter-feeders. *J. Mar. Sci. Eng.* **2022**, *10*, 607. [[CrossRef](#)]

**Disclaimer/Publisher’s Note:** The statements, opinions and data contained in all publications are solely those of the individual author(s) and contributor(s) and not of MDPI and/or the editor(s). MDPI and/or the editor(s) disclaim responsibility for any injury to people or property resulting from any ideas, methods, instructions or products referred to in the content.